

# Study of Oxidized-Porous Silicon as Insulating Film for HI-PS Field Emission Devices

Déborá A. C. Silva, Michel O. S. Dantas  
Centro de Engenharia, Modelagem e Ciências Sociais  
Universidade Federal do ABC  
Santo André, São Paulo, Brazil  
55 11 4996-8262  
michel.dantas@ufabc.edu.br

Elisabete Galeazzo, Henrique E.M. Peres,  
Francisco J. Ramirez-Fernandez  
Departamento de Engenharia de Sistemas Eletrônicos  
Universidade de São Paulo  
São Paulo, Brazil  
55 11 3091-5310

## ABSTRACT

This paper reports the study of Oxidized-Porous Silicon (Ox-PS) as insulating film for integrated Field Emission Devices (FE) fabricated by Hydrogen-Porous Silicon (HI-PS) technique. The PS thermal oxidation was conducted by varying process parameters such as temperature, time, and post-oxidation annealing. Morphological analysis by means of Fourier Transform-Infrared Spectrometry (FTIR) and optical microscopy indicated a fully oxidation of PS layers for all experimented process parameters. Metal-Oxide-Semiconductor (MOS) devices were fabricated to allow the electrical characterization of leakage current through Ox-PS from I-V curves. By applying the appropriated oxidation process parameters and post-oxidation annealing, a strong reduction of leakage current was characterized (from nA to pA) for the same bias level. This result indicates that Ox-PS obtained from suitable parameters is promising for use as insulating film in FE devices fabricated by HI-PS.

## Keywords

Oxidized Porous Silicon (Ox-PS), Field Emission Device (FE), HI-PS (Hydrogen Implant – Porous Silicon)

## 1. INTRODUCTION

Field emission devices (FE – devices that allows the electron extraction by applying of a strong electrical field in microstructures with singular tip geometry aspect) has been widely studied due their excellent electric characteristics such as low power consumption, high current density, room temperature operation, among others [1-3]. They are promising for applications based on devices known as “cold cathodes”: high-resolution optoelectronic systems, flat displays, x-ray sources, and gas sensing for example [4-8].

Several techniques and materials can be applied to obtain FE devices [5]; in special, silicon (Si) based FE are interesting due to the possibility of their integration with microelectronic circuit, which is promising for the development of miniaturized sensors. A technique named HI-PS (Hydrogen Implant – Porous Silicon) was proposed as a viable alternative to fabricate Si FE devices [9]. The advantages obtained with HI-PS include the use of compatible CMOS processes with low complexity to obtain the devices.

Despite the good results achieved with HI-PS technique, FE devices fabricated with integrated anode-cathode (which are basic structures of a FE device) in the same substrate present operational problems related to the poor electrical insulation between these two structures. PSG [10] and TiO<sub>2</sub> [11], among other dielectrics, can be used as insulator layers in FE devices, but silicon dioxide (SiO<sub>2</sub>) is the traditional material used with this

purpose since is totally compatible with CMOS processing [12-14]. All these insulators are generally obtained from CVD processes due to their relative large thicknesses (between 500 nm and 1 μm, depending on the size of the cathodes).

In the original HI-PS developed process, the electrical insulation is promoted by a SiO<sub>2</sub> film growth from dry thermal oxidation conducted with process times about 10 hours [9]. Even the relative large thickness of the SiO<sub>2</sub> film obtained in this process (about 1 μm) is not enough to guarantee an effective electrical insulation between anode-cathode structures, causing malfunction of the HI-PS FE device. Another relevant aspect is that the dimensions of cathode geometries obtained by HI-PS (with height about 10 μm) demand insulating films with the same order of magnitude, which difficult or even prevents the use of these traditional materials and processes.

One proposed alternative to solve this problem could be the use of Oxidized Porous Silicon (Ox-PS) layers as insulator. The Ox-PS, due to its singular properties, is explored in several applications such humidity sensing based on nanotechnology, electrical insulation in microwave devices and integrated circuits based on SOI technology, among others [15-20].

The oxidation parameters applied to form Ox-PS are quite distinct when compared with the consolidated SiO<sub>2</sub> films: high thickness PS layers (about tens of micrometers) can be fully oxidized with relative short process times (about tens of minutes) and with temperatures lower than 1000° C. It is possible due to its large inner surface and high reactivity with oxidant species [18]. Another remarkable characteristic is the possibility to obtain dielectric constant *K* values closer to the SiO<sub>2</sub> (about 3.8) depending on the anodization parameters applied to obtain PS [15, 17]. Nevertheless, the most attractive aspect is that Ox-PS is obtained from Si substrates with PS layers, which are the basis of the HI-PS processing, thus, it could be incorporated in the FE fabrication process without introducing additional complexity or cost.

Based on the exposed, this work focuses on the study of Ox-PS for applications as insulating film layer between the anode and cathode structures in FE devices obtained by HI-PS, aiming to reduce the leakage current from the bulk to the anode, and promoting consequently an effective electron emission current from the cathodes.

## 2. EXPERIMENTAL PROCEDURE

As described before, Ox-PS is formed from oxidation of PS layers, which were obtained in this work by anodization of Si wafers as follows: first, BF<sub>2</sub><sup>+</sup> ions were implanted at the backside of p type Si wafers (<100>, ρ = 10-20 Ω.cm); second, they were annealed (parameters: T = 900° C, t = 30 minutes, N<sub>2</sub> environment) to promote ohmic contact (necessary to the

electrochemical process); third, anodization was conducted to form PS layers (parameters:  $T = 40^{\circ}\text{C}$ ,  $t \cong 14$  minutes, concentrated HF solution (49% wt)).

After anodization, the PS layers were thermally oxidized in dry  $\text{O}_2$  environment by varying the oxidation conditions (A, B, C and D) as described in Table 1. A post-oxidation annealing ( $T = 750^{\circ}\text{C}$ ,  $t = 120$  minutes, “Forming Gas” environment) was also experimented in some samples to verify the improvement of dielectric characteristics.

Optical microscopy and Fourier Transform-Infrared Spectrometry (FTIR) were used to evaluate the morphology. For the electrical characterization, an aluminum layer (300nm thick) was deposited and photolithographed over Ox-PS layers to obtain MOS devices, and the leakage current was analyzed from I-V curves measured with a HP4156 Semiconductor Parameter Analyzer.

**Table 1. Oxidation Parameters**

Oxidation Condition	Temperature ( $T = ^{\circ}\text{C}$ )	Time ( $t = \text{minutes}$ )	Post-oxidation annealing
A	800	20	_____
B	1000	20	_____
C	1000	60	_____
D	1000	60	$T = 750^{\circ}\text{C}$ $t = 120 \text{ min.}$ “Form. Gas”

### 3. RESULTS AND DISCUSSION

#### 3.1 Morphological Analysis

Figure 1(a) shows optical microscopy images of the sample surfaces before and after oxidation of PS. All adopted temperatures and times were apparently enough to promote total oxidation of PS layers. No thickness variations of the layers were verified before (Figure 1(b)) and after oxidation (Figure 1(c)), but surface cracks were observed in samples oxidized in the temperature of  $800^{\circ}\text{C}$  (Figure 1(d)), preventing these samples to be electrically characterized. Small cracks were observed on samples oxidized in the temperature of  $1000^{\circ}\text{C}$  for 20 minutes, and they were completely avoided in the samples oxidized in the same temperature ( $T = 1000^{\circ}\text{C}$ ), but with oxidation time increased (60 minutes – Figure 1(e)). These results indicate that temperatures below  $1000^{\circ}\text{C}$  or fast oxidation times can introduce mechanical stress in the Ox-PS layers, promoting their crack.

FTIR spectrometry was used to verify if the oxidation parameters were effective to promote total oxidizing of the PS layers. Figure 2 shows the spectra obtained. The curve (a) of Figure 2 presents the typical as formed PS spectrum [21], where the presence of peaks related to silicon-hydrogen bonds is noted:  $\text{Si-H}_3$  “bending” ( $628 \text{ cm}^{-1}$ ),  $\text{Si-H}_2$  ( $2100\text{-}2108 \text{ cm}^{-1}$ ),  $\text{Si-H}_2$  “wagging” ( $665 \text{ cm}^{-1}$ ) and  $\text{Si-H}_2$  “scissors bending” ( $910\text{-}916 \text{ cm}^{-1}$ ) [22]. The presence of silicon-oxygen bonds ( $\text{Si-O}$  ( $1160 \text{ cm}^{-1}$ ),  $\text{Si-O-Si}$  “asymmetric stretching” ( $984 \text{ cm}^{-1}$ ) and  $\text{Si-O-Si}$  “stretching” ( $1070 \text{ cm}^{-1}$ )) occurs because the high reactivity of this material to environment exposure.

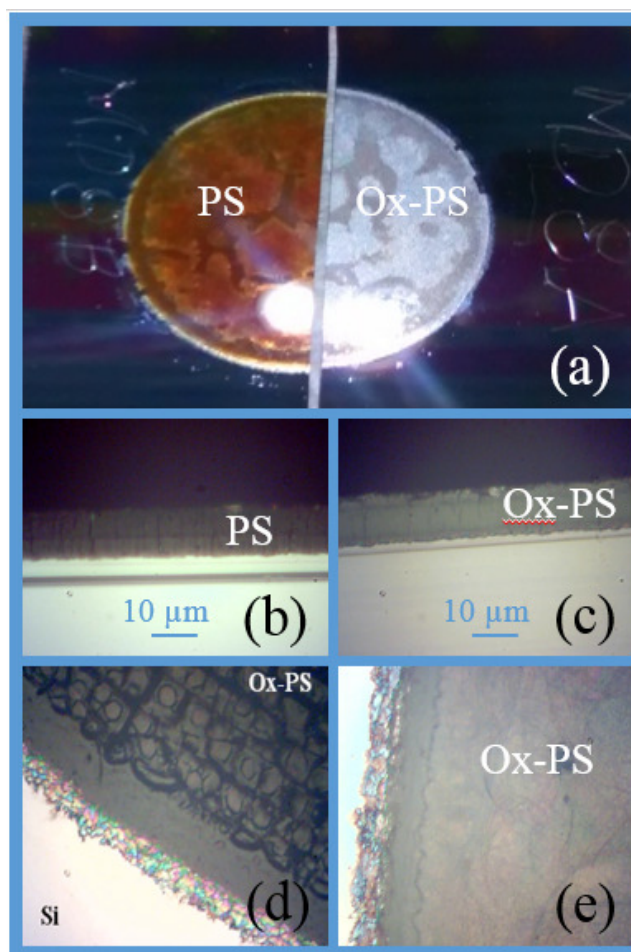


**Figure 1. (a) Sample split showing PS (left) and Ox-PS (right) obtained with  $T = 1000^{\circ}\text{C}$  and  $t = 20$  minutes. (b) Cutaway view of PS layer and (c) Ox-PS layer ( $T = 1000^{\circ}\text{C}$  and  $t = 20$  minutes). (d) Cracks on sample oxidized with  $T = 800^{\circ}\text{C}$  and  $t = 20$  minutes. (e) Sample without cracks evidence, oxidized with  $T = 1000^{\circ}\text{C}$  and  $t = 60$  minutes.**

The Ox-PS (Figure 2 (b-e) spectra) shows the complete elimination of silicon-hydrogen bonds, the increasing of silicon-oxygen bonds ( $\text{Si-O}$  ( $1160 \text{ cm}^{-1}$ ),  $\text{Si-O-Si}$  “asymmetric stretching” ( $984 \text{ cm}^{-1}$ ) and  $\text{Si-O-Si}$  “stretching” ( $1070 \text{ cm}^{-1}$ )), and the emergence of peaks related to “new” silicon-oxygen bonds:  $\text{SiO}_x$  ( $450 \text{ cm}^{-1}$ ),  $\text{Si-O-Si}$  ( $470 \text{ cm}^{-1}$ ) and  $\text{Si-O-Si}$  “symmetric stretching” ( $810 \text{ cm}^{-1}$ ) [22-24]. The wide “cut at the top” peaks noted between  $984 \text{ cm}^{-1}$  and  $1210 \text{ cm}^{-1}$  (related to silicon-oxygen bonds) indicate the saturation of IR detector due to the relative large thickness of Ox-PS layers (about  $10 \mu\text{m}$ ).

The Ox-PS spectrum of the sample oxidized with  $T = 800^{\circ}\text{C}$  and  $t = 20$  minutes (Figure 2, (b) spectrum) shows a little peak referent to carbon type bonds ( $\text{Si-CH}_3$  ( $1640 \text{ cm}^{-1}$ )), probably due to the sample handling. In summary, the replacement of typical PS silicon-hydrogen type bonds for silicon-oxygen type bonds in all oxidized samples indicates that the parameters adopted were effective to promote total oxidation of PS layers.

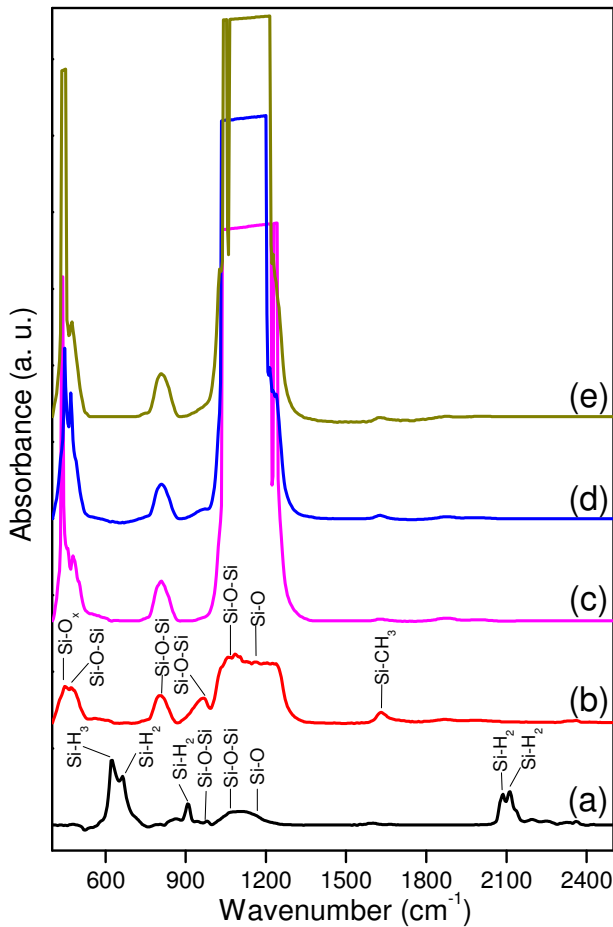


**Figure 2.** FTIR spectra of (a) PS reference and Ox-PS processed with the following parameters: (b)  $T = 800^\circ\text{C}$  and  $t = 20\text{ min}$ , (c)  $T = 1000^\circ\text{C}$  and  $t = 20\text{ min}$ , (d)  $T = 1000^\circ\text{C}$  and  $t = 60\text{ min}$ , and (e)  $T = 1000^\circ\text{C}$ ,  $t = 60\text{ min}$  + thermal annealing in forming gas environment.

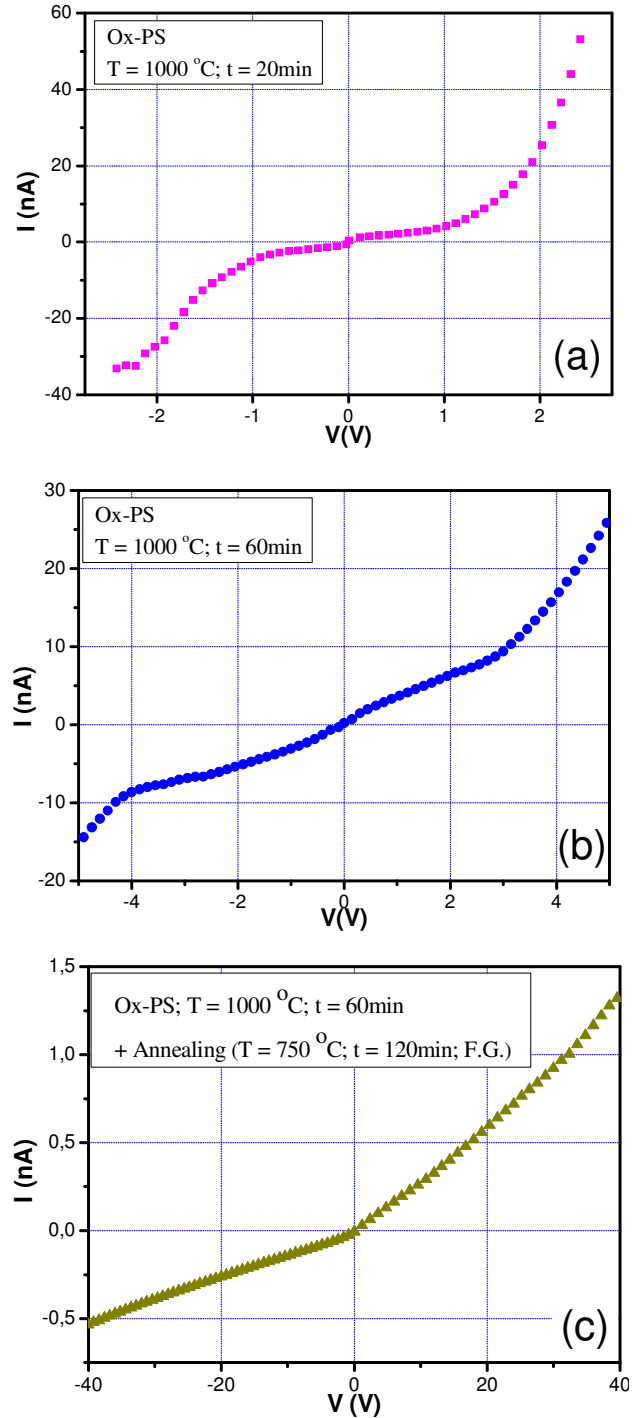
### 3.2 Electrical Characterization

Figure 3 shows I-V curves measured for the MOS devices fabricated from Ox-PS layers obtained with  $T = 1000^\circ\text{C}$ . A typical Schottky electrical behavior is noted, which characterizes the semiconductor nature of the metal-oxide contact.

A leakage current about 60 nA was measured for an applied potential of 2.5 V in the device obtained with oxidation time of 20 minutes (Figure 3(a)), which is a current value relatively high for application of this oxide as insulating film in HI-PS FE device. The current level was reduced to about 7.5 nA (for the same level of applied potential (2.5 V)) in the device with oxidation time of 60 minutes (Figure 3(b)), which demonstrates that increased oxidation times can promote more densification of the films and, consequently, improve their dielectric characteristics.

Figure 3(c) shows the I-V curve obtained for the device submitted to the post-oxidation annealing (applied in the samples with better morphologic and electric characteristics (i.e. samples oxidized with  $T = 1000^\circ\text{C}$  and  $t = 60\text{ min}$ )), where we can note a strong reduction of leakage current (from 7.5 nA to ~50 pA) for the same bias level as compared with the other experimented samples. The maximum current value measured was about 1.4 nA, characterized for an applied potential of 40 V, which corresponds

to the voltage compliance of the equipment used in this analysis. The hypothesis for the reduction of the leakage current after thermal annealing is the passivation of trapped and free charges present in the oxide [25]. These results demonstrate that the Ox-PS obtained under Oxidation Condition D ( $T = 1000^\circ\text{C}$ ,  $t = 60\text{ min}$  and thermal annealed) is suitable for use as insulating film in HI-PS FE integrated device.



**Figure 3.** I-V curves from MOS devices applying Ox-PS as insulating between metal (aluminum) and semiconductor (Si p type).

## 4. CONCLUSIONS AND PERSPECTIVE

Thermal conditions were analyzed to promote total oxidation of PS layers. Short oxidation times (20 minutes) and low temperatures ( $T = 800\text{ }^{\circ}\text{C}$ ) introduced mechanical stress in the Ox-PS films. The increase of temperature and oxidation time ( $T = 1000\text{ }^{\circ}\text{C}$  and  $t = 60$  minutes) has avoided this problem, and allowed the obtaining of oxidized PS films free of cracks.

FTIR analysis showed the complete oxidation of PS films for all experimented oxidation conditions, which was demonstrated by the transition or replacement of silicon-hydrogen bonds to silicon-oxygen type bonds. The electrical characterization presented a reduction of the leakage current when the time of oxidation was increased from 20 minutes to 60 minutes in  $1000^{\circ}\text{C}$ , but the current value obtained with low bias (about  $7.5\text{ nA}$  for  $2.5\text{ V}$  of applied voltage) was not suitable for FE applications. After a thermal annealing process, the leakage current was strongly decreased (from  $\text{nA}$  to about  $50\text{ pA}$ ) for the same bias level, probably due to the passivation of charges present on porous oxide structure.

In conclusion, the preliminary Ox-PS results, obtained with temperatures of  $1000\text{ }^{\circ}\text{C}$ , times of 60 minutes, and submitted to post-oxidation thermal annealing process, has potential for applications as insulating films in FE devices fabricated by HI-PS. As perspective, these oxidation conditions will be applied in the HI-PS process to obtain integrated anode-cathode structures. This implementation aims, besides the proper electrical insulation, the reduction of process steps and complexity of this technique.

## 5. ACKNOWLEDGMENTS

The authors would like to thank the *Laboratório de Sistemas Integráveis* (LSI) for thermal annealing of samples after  $\text{BF}_2^+$  implant, *Central Experimental Multiusuário* (CEM) for FTIR analysis, and UFABC scholarship.

## 6. REFERENCES

- [1] G. Bedo, W. Kraus, and R. Muller, "Comparison of different micromechanical vacuum sensors", *Sensors and Actuators A*, vol. 85, pp. 181–188, August 2000.
- [2] S. Ghionea, D. Hull, and K. Williams, "Characterization techniques for a MEMS electric-field sensor in vacuum", *Journal of Electrostatics*, vol. 71, pp. 1076–1082, December 2013.
- [3] Z. Hou et al., "A MEMS-Based ionization gas sensor using carbon nanotubes", *IEEE Transactions on Electron Devices*, v. 54, pp. 1545–1548, June 2007.
- [4] D.L.J. She, S. Xu, and S. Deng, "Zinc oxide nanowire lateral field emission devices and its application as display pixel structures", *IEEE Transactions on Electron Devices*, v. 60, pp. 2924–2930, July 2013.
- [5] G.N. Fursey, "Field emission in vacuum microelectronics", *Applied Surface Science*, vol. 215, pp. 113–134, June 2003.
- [6] W. Shim et al., "Hard-tip, soft-spring lithography", *Nature*, vol. 469, pp. 516–520, January 2011.
- [7] S. Wilfert and C. Edelmann, "Field emitter-based vacuum sensors", *Vacuum*, vol. 86, pp.556–571, January 2012.
- [8] S. Cheng, F.A. Hill, E.V. Heubel, and L.F. Velasquez-Garcia, "Low-bremsstrahlung x-ray source using a low-voltage high-current-density nanostructured field emission cathode and a transmission anode for markerless soft tissue imaging", *Journal of Microelectromechanical Systems*, vol. 24, pp. 373–383, July 2014.
- [9] M.O.S. Dantas, E. Galeazzo, H.E.M. Peres, M.M. Kopelvyk and F.J. Ramirez-Fernandez, "Silicon field-emission devices fabricated using the hydrogen implantation - porous silicon (HI-PS) micromachining technique", *Journal of Microelectromechanical Systems*, vol. 17, pp. 1263–1269, December 2008.
- [10] J.T. Trujillo and C.E. Hunt, "Fabrication of gated silicon field-emission cathodes for vacuum microelectronics and electron-beam applications", *Journal of Vacuum Science & Technology B*, vol. 11, pp. 454–458, April 1993.
- [11] J. Koohsorkhi, S. Mohajezadeh, and S. Darbari, "Investigation of carbon nanotube-based field-emission triode devices on silicon substrates", *IEEE Transactions on nanotechnology*, vol. 11, pp. 1252–1258, November 2012.
- [12] A. Basu, M.E. Swanwick, A.A. Fomani, and L.F. Velásquez-García, "A portable x-ray source with a nanostructured Pt-coated silicon field emission cathode for absorption imaging of low-Z materials", *Journal of Physics D: Applied Physics*, vol. 48, pp. 1–11, May 2015.
- [13] G. Pirio et al., "Fabrication and electrical characteristics of carbon nanotube field emission microcathodes with an integrated gate electrode", *Nanotechnology*, vol. 13, pp. 1–4, January 2002.
- [14] M. Ding, G. Sha, and A.I. Akinwande, "Silicon field emission arrays with atomically sharp tips: turn-on voltage and the effect of tip radius distribution", *IEEE Transactions on electron devices*, vol. 49, pp. 2333–2342, December 2002.
- [15] D. Molinero et al., "Properties of oxidized porous silicon as insulator material for RF applications", *Spanish Conference on Electron Devices*, pp. 131–133, February 2005.
- [16] R.P. Holmstrom and J.Y. Chi, "Complete dielectric isolation by highly selective and selfstopping formation of oxidized porous silicon", *Applied Physics Letters*, vol. 42, pp. 386–388, January 1983.
- [17] S. Shieh and J.W. Evans, "Some preliminary observations of the rapid thermal oxidation of porous silicon, and the rapid thermal nitriding of oxidized porous silicon", *Journal of Vacuum Science & Technology B*, vol. 12, p.1422–1426, March 1994.
- [18] J. Riikonen et al., "Surface chemistry, reactivity, and pore structure of porous silicon oxidized by various methods", *Langmuir*, vol. 28, pp. 10573–10583, June 2012.
- [19] A. Pap et al., "Thermal oxidation of porous silicon: study on structure", *Applied Physics Letters*, vol. 86, pp.041501-1- 3, January 2005.
- [20] H. Takai and T. Itoh, "Porous silicon layers and its oxide for the silicononinsulator structure", *Journal of Applied Physics*, vol. 60, pp. 222–225, March 1986.
- [21] Q. Hong, C. Rogero, J.H. Lakey, B.A. Connolly, A. Houlton, and B.R. Horrocks, "Immobilisation of proteins at silicon surfaces using undecenylaldehyde: demonstration of the retention of protein functionality and detection strategies", *Analyst*, vol. 134, pp. 593–601, January 2009.
- [22] E. Galeazzo, Silício Poroso para Aplicações em Sensores e Microsistemas, Thesis, Universidade de São Paulo, 2000.
- [23] N.F. Wang et al., "Porous  $\text{SiO}_2/\text{MgF}_2$  broadband antireflection coatings for superstrate-type silicon-based tandem cells", *Optics Express*, vol. 20, pp. 7445–7453, March 2012.
- [24] D.B. Mawhinney, J.A. Glass, and J.T. Yates, "FTIR study of the oxidation of porous silicon", *Journal of Physical Chemistry B*, vol. 101, pp. 1202–1206, February 1997.
- [25] J.A. Felix et al., "Charge trapping and annealing in high-K gate dielectrics". *IEEE Transactions on Nuclear Science*, vol. 51, pp. 3143–3149, December 2004.